Cleveland State University
EngagedScholarship@CSU

Chemical & Biomedical Engineering Faculty Publications

Chemical & Biomedical Engineering Department

12-2003

Effect of Crucible Diameter Reduction on the Convection, Macrosegregation, and Dendritic Morphology During Directional Solidification of Pb-2.2 Wt Pct Sb Alloy

Follow this and additional works at: https://engagedscholarship.csuohio.edu/encbe_facpub

Part of the Materials Science and Engineering Commons

How does access to this work benefit you? Let us know!

Jun Chen
Cleveland State University

Surendra N. Tewari
Cleveland State University

G. Magadi
American Bureau of Shipping

H. C. DeGroh III
NASA-Glenn Research Center

Publisher's Statement

Copyright 2003 ASM International. This paper was published in Metallurgical and Materials Transactions A: Physical Metallurgy and Materials Science, Vol. 34A, Issue 12, pp. 2985-2990 and is made available as an electronic reprint with the permission of ASM International. One print or electronic copy may be made for personal use only. Systematic or multiple reproduction, distribution to multiple locations via electronic or other means, duplications of any material in this paper for a fee or for commercial purposes, or modification of the content of this paper are prohibited.

Available on publisher's site at: http://www.springerlink.com/content/9364865t205316m2/.

Original Citation

Chen, J., Tewari, S.N., Magadi, G., & DeGroh, H.C. (2003). Effect of Crucible Diameter Reduction on the Convection, Macrosegregation, and Dendritic Morphology During Directional Solidification of Pb-2.2 Wt Pct Sb Alloy. Metallurgical and Materials Transactions A: Physical Metallurgy and Materials Science **34A**, 2985-2990.

Repository Citation

Chen, Jun; Tewari, Surendra N.; Magadi, G.; and DeGroh, H. C. III, "Effect of Crucible Diameter Reduction on the Convection, Macrosegregation, and Dendritic Morphology During Directional Solidification of Pb-2.2 Wt Pct Sb Alloy" (2003). *Chemical & Biomedical Engineering Faculty Publications*. 10.
https://engagedscholarship.csuohio.edu/encbe_facpub/10

This Article is brought to you for free and open access by the Chemical & Biomedical Engineering Department at EngagedScholarship@CSU. It has been accepted for inclusion in Chemical & Biomedical Engineering Faculty Publications by an authorized administrator of EngagedScholarship@CSU. For more information, please contact library.es@csuohio.edu.

Effect of Crucible Diameter Reduction on the Convection, Macrosegregation, and Dendritic Morphology during Directional Solidification of Pb-2.2 Wt Pct Sb Alloy

JUN CHEN, S.N. TEWARI, G. MAGADI, and H.C. DE GROH III

The Pb-2.2 wt pct Sb alloy has been directionally solidified in 1-, 2-, 3-, and 7-mm-diameter crucibles with planar and dendritic liquid-solid interface morphology. For plane front solidification, the experimentally observed macrosegregation along the solidified length follows the relationship proposed by Favier.[17,18] Application of a 0.4 T transverse magnetic field has no effect on the extent of convection. Reducing the ampoule diameter appears to decrease the extent of convection. However, extensive convection is still present even in the 1-mm-diameter crucible. An extrapolation of the observed behavior indicates that nearly diffusive transport conditions require ampoules that are about 40 μm in diameter. Reduction of the crucible diameter does not appear to have any significant effect on the primary dendrite spacing. However, it results in considerable distortion of the dendrite morphology and ordering. This is especially true for the 1-mm-diameter samples.

I. INTRODUCTION

AT low growth speed and high thermal gradient, the liquid-solid interface is planar during directional solidification of binary alloys. It first becomes cellular and then dendritic as the growth speed increases. It has now been well established that convection influences the planar-to-cellular transition[1–4] and the primary cellular/dendritic spacings.[5,6,7] During upward directional solidification, the thermal profile in the melt provides stability against convection because the melt density decreases with increasing temperature. However, the solutal profile in the melt is stabilizing only for those alloys where the increased solute content results in increased melt density, for example, hypoeutectic aluminum-copper alloy. Even for these alloys the radial thermal gradient at the triple junction of the solid-liquid interface and the ampoule wall causes mild convection that is localized in the vicinity of the liquid-solid interface.[8,9] The solutal profile in the melt is destabilizing for those alloys in which the melt density decreases with increased solute content, for example, hypoeutectic lead-antimony. This solutal gradient can cause extensive convection in the overlying and the interdendritic melt and result in a severe macrosegregation along the solidified length for the planar, cellular, or dendritic morphologies.[10,11]

Since most theoretical dendrite growth and morphology models consider only diffusive thermal and solutal transports, attempts have been made to eliminate convection to enable a quantitative comparison of predictions with experimental observations.[9,12] In a recent study, it has been shown that reducing the ampoule diameter to about 1 mm almost completely eliminates convection during directional solidification of Al-4 wt pct Cu alloy.[8,9] The purpose of this research was to examine if similar reduction in the ampoule diameter can reduce the more intense, longer range, convection that occurs during directional solidification of Pb-2.2 wt pct Sb.

JUN CHEN, Graduate Student, and S.N. TEWARI, Professor, are with the Chemical Engineering Department, Cleveland State University, Cleveland, OH 44115. Contact e-mail: s.tewari@csuohio.edu G. MAGADI, formerly Research Associate, Chemical Engineering Department, Cleveland State University, is Senior Engineer, Materials Department, American Bureau of Shipping, Houston, TX 77060-6008. H.C. DE GROH III, Scientist, is with the Advanced Metallics Branch, NASA–Glenn Research Center, Cleveland, OH 44135.

Manuscript submitted June 25, 2002.

II. EXPERIMENTAL PROCEDURE

A. *DS Furnace*

Since the directional solidification furnace is described earlier,[10,11] only a brief description of its operation will be presented here. To accomplish directional solidification and avoid convection, the furnace assembly is translated and the sample is held stationary. In addition, the entire assembly sits on top of a vibration isolation platform. Samples are kept in quartz ampoules and are directionally solidified in a flowing argon atmosphere. The furnace is initially translated downward to remelt the cast alloy feed stock and about 1-cm length of a 5-cm long single-crystal lead seed (length parallel to [100]) kept at the bottom. The furnace is then translated upward to achieve the directional solidification. After solidifying for about 10 cm, the rest of the melt column is quenched by withdrawing the furnace quickly and blasting the ampoule surface with helium gas flowing through a liquid nitrogen tank.

B. *Precasting of Capillary Samples*

Cast Pb-2.2 wt pct Sb feed stock cylinders were placed into a quartz directional solidification ampoule (7-mm i.d.) on top the single-crystal seed. The ampoule also contained a bundle of 1-, 2-, and 3-mm i.d. quartz capillaries that were connected to a vacuum setup. The furnace was first lowered in order to melt the charge and about 1-cm portion of the seed. A 20- to 22-cm long melt column was then sucked into the capillaries by inserting the capillary bundle into the melt and activating the vacuum suction. The capillaries were further lowered until their bottom was near the liquid-solid

U.S. GOVERNMENT WORK
NOT PROTECTED BY U.S. COPYRIGHT

interface and the entire assembly was directionally solidified at 10 μm s^{-1} for a distance of about 5 cm. This method of casting provided about 4-cm-long directionally solidified solid portion at the bottom of the capillaries that was parallel to [100]. This ensures that during subsequent re-melting and directional solidification, the precast capillary samples will grow along [100].

C. *Planar Liquid-Solid Interface*

The precast 1-, 2-, and 3-mm i.d. capillary samples were bundled together and kept inside another 7-mm i.d. quartz ampoule. The capillary bundle was surrounded by gallium metal kept in the 7-mm i.d. ampoule in order to ensure that all of the samples solidified under identical thermal conditions. After remelting an approximately 14-cm-long portion (leaving about 3-cm-long [100] oriented solid at the bottom), the capillary samples were directionally solidified at 0.4 μm s^{-1} with a thermal gradient of 82 K cm^{-1}.

Two 7-mm-diameter samples were also directionally solidified at 120 K cm^{-1} and a growth speed of 0.4 μm s^{-1} in order to examine the influence of transverse magnetic field on convection. One sample was grown in the presence of a 0.4 T transverse magnetic field, and the other without the field.

D. *Dendritic Liquid-Solid Interface*

The capillary samples with dendritic morphologies were obtained by directional solidification at 3 and 30 μm s^{-1} with a thermal gradient of 82 K cm^{-1}. The growth speed of 3 μm s^{-1} corresponds to the dendrites in the vicinity of the cell-to-dendrite transition, whereas the 30 μm s^{-1} corresponds to well-branched fully dendritic regime.

E. *Macrosegregation and Metallography*

The directionally solidified samples were sectioned along the directionally solidified length to obtain about 2- to 5-mm-thick slices, depending on the sample diameter, for chemical analysis by atomic absorption spectroscopy. An approximately 2-cm-long portion of the sample in the vicinity of the quenched liquid-solid interface was used for optical metallography.

III. RESULTS

A. *Plane Front Solidification*

1. *Influence of transverse magnetic field*

Figure 1(a) shows the variation in antimony content as a function of solidification distance for the Pb-2.2 wt pct Sb sample grown in the 7-mm-i.d. ampoules with and without the application of magnetic field. The open symbols indicate the compositions in the quenched liquid portion of the specimen. Both the samples show extensive longitudinal macrosegregation, an indication of the strong convection present in the samples.

Figure 1(b) plots the macrosegregation data as a function of the fraction distance solidified for both the samples, with and without the application of transverse magnetic field, where C_s is the solute content after directional solidification and C_0 is the initial solute content of the alloy. The macrosegregation pattern clearly indicates that the solutal redistribution is not diffusive. The profiles are typically those expected from plane front solidification of a well-mixed alloy melt. Almost identical solutal segregation profiles indicate that the application of a 0.4 T transverse magnetic field has no influence on the convection.

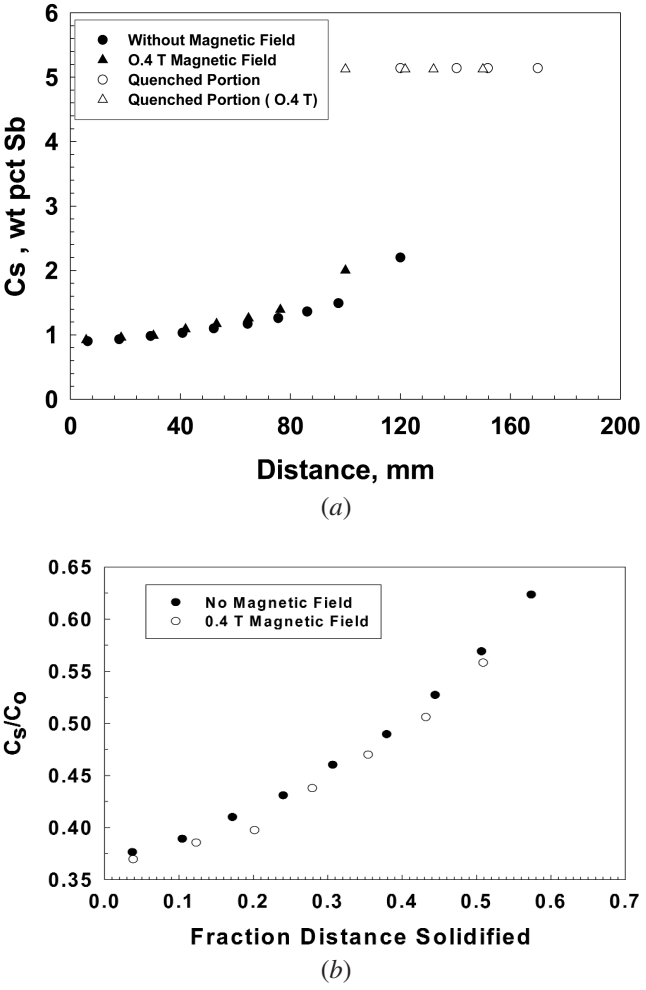

Fig. 1—Macrosegregation along directionally solidified length of Pb-2.2 wt pct Sb alloy samples grown in 7-mm-i.d. crucibles at 0.4 μm s^{-1} and 120 K cm^{-1}. One sample was grown in the presence of a transverse magnetic field of 0.4 T, and the other without it. (*a*) Variation in the antimony content (C_s) as a function of solidification distance. Open symbols are for the quenched portion of the sample. (*b*) C_s/C_0 *vs* fraction distance solidified.

2. *Effect of reducing the ampoule diameter*

Figure 2 compares the dimensionless composition profile as a function of fraction distance solidified for the 1-, 2-, 3-, and 7-mm-diameter samples that were directionally solidified with a planar liquid-solid interface. For a diffusive transport, one would expect a steady-state value of unity for the C_s/C_0 after an initial transient during which the antimony content increases from k_0C_0, where k_0, the solute partition coefficient, is 0.3.[13] The length of the transient would be expected to be D_l/Rk_0, where D_l is the diffusivity of antimony in the Pb-2.2 wt pct Sb alloy melt (1.13×10^{-5} cm^2 s^{-1} at 585 K[14]) and R is the growth speed, 0.4 μm s^{-1}. For our growth condition, D_l/Rk_0 is 0.9 cm, which in Figure 2 corresponds to about 0.06 fraction distance

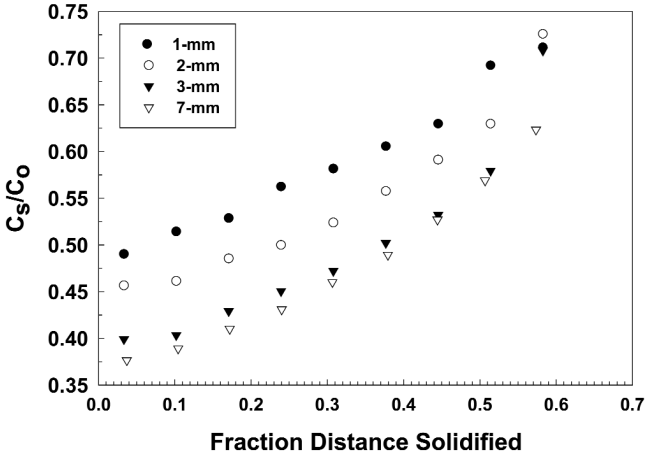

Fig. 2—Influence of reducing the ampoule diameter on the longitudinal macrosegregation in directionally solidified Pb-2.2 wt pct Sb alloy samples. The 1-, 2-, and 3-mm samples were grown at 0.4 μm s^{-1}, 82 K cm^{-1}, while the 7-mm sample was grown at 0.4 μm s^{-1}, 120 K cm^{-1}.

solidified. Since the minimum slice thickness required for chemical analysis was about 0.5 cm, the very initial solute content k_0C_0 is not seen in Figure 2. The solutal profiles in Figure 2 are clearly not those expected from a diffusive mass transport. Their segregation pattern indicates extensive convection and mixing during directional solidification. The extent of macrosegregation, however, shows a systematic decrease with the decreasing ampoule diameter. This indicates that the intensity of convection decreases with decreasing ampoule diameter.

B. *Primary Dendrite Spacing and Morphology*

1. *Morphology and disorder*

Figure 3 shows the transverse microstructures of the Pb-2.2 wt pct Sb samples grown in 1-, 2-, 3-, and 7-mm-diameter crucibles at 30 μm s^{-1}. The extent of dendrite disorder appears to increase with decreasing sample diameter in spite of the fact that they were all grown from the same single crystal seed. The 1-, 2-, and 3-mm-diameter samples not only had the same seed but they were also directionally solidified together, as one bundle, under identical growth conditions. Yet, the 1-mm-diameter sample has a much poorer dendrite ordering and alignment compared with the 3-mm sample.

Figure 4 shows the frequency distribution of the number of nearest neighbors in the 1-, 2-, 3-, and 7-mm samples grown at 30 μm s^{-1}. The number of nearest neighbors was obtained by constructing Voronoi polygons in a manner described in Reference 15. The solid curves are the Gaussian fit through the data points. The figures also show the corresponding Gaussian fit parameters: A_0, the peak height, A_1, the center, and A_2, the width. There is a dominance of six neighbors. However, significant fractions of dendrites, about 40 pct for the 7-mm-diameter sample and about 70 pct for the 1-mm-diameter sample, do not have six neighbors. One should, however, note that there are only about 20 dendrites in the 1-mm sample. A small number of dendrites coupled with the fact that dendrites at the crucible wall are affected by the wall effects do not allow an accurate statistical comparison. However, it is apparent that the most probable number of nearest neighbors (A_1) increases in the following order: 5.3, 5.6, 5.9, and 6.0 for crucible diameters of 1, 2, 3, and 7 mm, respectively. This suggests that a decrease in the crucible diameter results in increased distortion in the ordering of primary dendrites.

2. *Primary dendrite spacing*

Figure 5 shows the average primary dendrite spacing in the samples grown at 3 and 30 μm s^{-1}. The mean and standard deviation values of primary spacing were obtained by minimum spanning tree analysis of dendrite centers, as described in Reference 15. The mean spacing ranges from 175 to 180 μm for the 3 μm s^{-1} samples, and from 142 to 151 μm for the 30 μm s^{-1}. There does not appear to be any systematic influence of the ampoule diameter on the primary dendrite spacing for the 3 μm s^{-1} samples; the ranges are overlapping with each other (Figure 5). However, at the higher growth speed of 30 μm s^{-1}, there appears to be a systematic increase in the primary spacing with decreasing ampoule diameter.

These primary dendrite spacings are significantly smaller than those predicted by the Hunt-Lu model[16] for the purely diffusive mass-transport conditions. The ratio of the experimentally observed and the theoretically predicted spacing is about 0.32 for the 3 μm s^{-1}, and about 0.65 for the 30 μm s^{-1} samples. As mentioned earlier, the 3 μm s^{-1} growth is in the dendritic regime near the cell-to-dendrite transition, where the side branches are not as well developed, compared to the 30 μm s^{-1} sample that is grown in the well-branched dendrite regime. The mushy zone is, therefore, less permeable for the 30 μm s^{-1} samples as compared with the 3 μm s^{-1} ones. The more intense convection in the 3 μm s^{-1} sample may be responsible for the observed larger deviation from the theoretical prediction for this growth speed compared with 30 μm s^{-1}; convection is believed to reduce primary dendrite spacings.[6]

The observation in Figure 5 that primary spacing in the 1-mm sample is larger than that in the 3-mm one, at the higher growth speed of 30 μm s^{-1}, suggests that decreasing ampoule diameter may be reducing the extent of mushy-zone convection. The suppression in the convection is, however, not as effective at the lower growth speed of 3 μm s^{-1}, where reduction in the crucible diameter does not have any influence on primary spacing.

IV. DISCUSSION

Plane front directional solidification in the presence of purely diffusive mass transport results in a crystal of nearly uniform composition except for the initial and final transients. The initial transient is formed while the solute boundary layer builds up from a liquid composition at the interface of C_0 to its steady-state value of C_0/k_0 and the solidification distance required to reach the steady state is approximately equal to D_l/Rk_0. In the presence of convective mixing, a diffusion boundary layer of thickness δ is often assumed, outside of which liquid composition is uniform due to convection and inside of which mass transport is by diffusion only. Favier[17,18] developed an analytical model in terms of the parameter $\Delta = \delta R/D_l$ in order to describe the composition profile for the entire growth regime, from purely diffusive to completely convective. During the

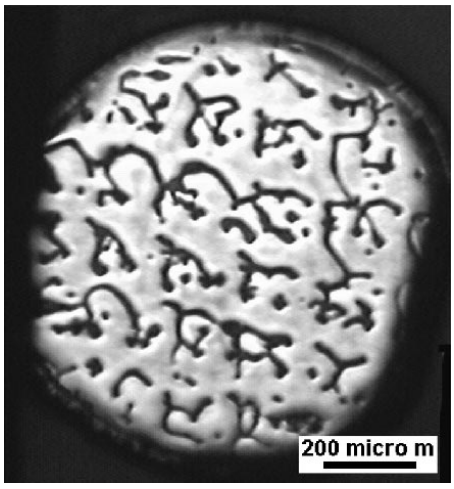

(*a*)

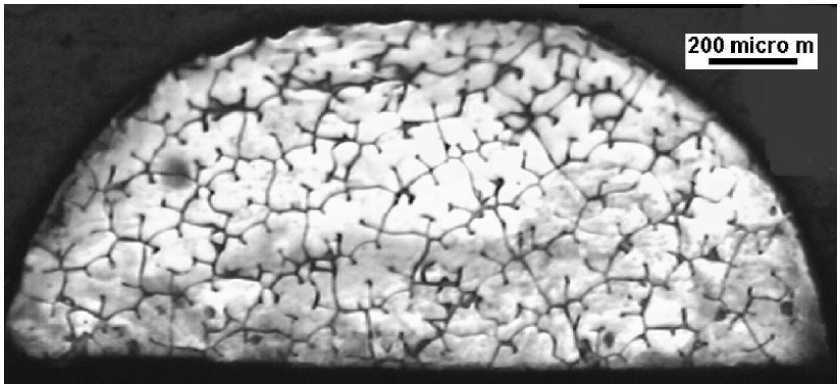

(*b*)

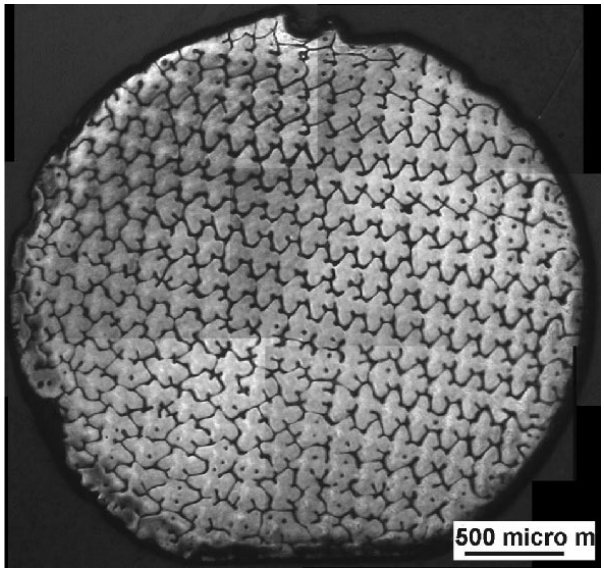

(*c*)

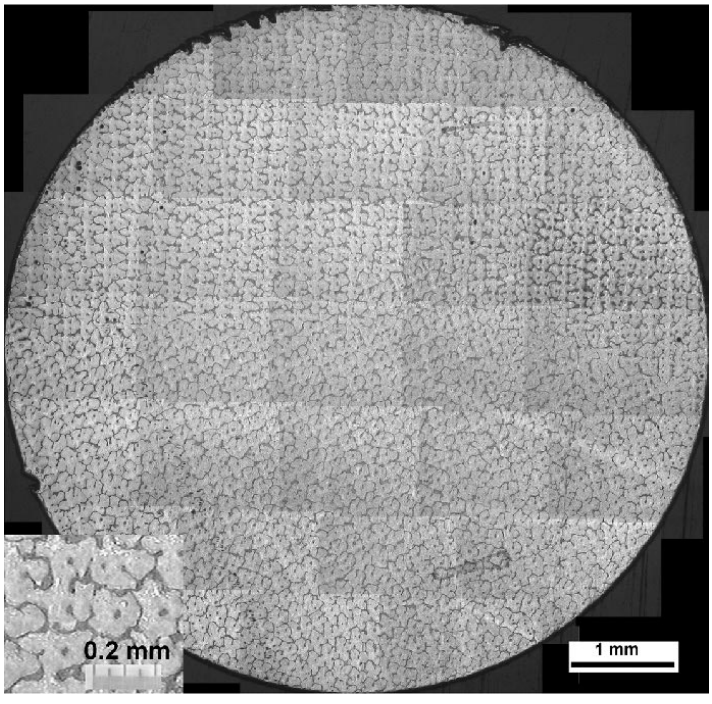

(*d*)

Fig. 3—Transverse microstructures of Pb-2.2 wt pct Sb samples directionally solidified at 30 μm s^{-1} in the crucible of diameters: (*a*) 1 mm, (*b*) 2 mm, (*c*) 3 mm, and (*d*) 7 mm. The 7-mm sample was grown at a thermal gradient of 120 K cm^{-1}, and the rest were grown at 82 K cm^{-1}.

initial transient, $C_s(x)/C_0 = k(\Delta)[1 - A_1(\Delta) \exp(-\beta_1 Rx/4D_l)]$, where

$$A_1(\Delta) = 8(1 - k_0)[k_0 + (1 - k_0) \exp(-\Delta)] \sin^2 \alpha_1 / [\Delta\beta_1(\Delta)(1 - 2\cos^2 \alpha_1/((1 - 2k_0)\Delta)].$$

Here, $\beta_1 = 1 + (1 - 2k_0)^2 tg^2 \alpha_1$, and α_1 can be obtained by the following equation:

$$2\alpha_1 \cos \alpha_1 - (1 - 2k_0)\, \Delta \sin \alpha_1 = 0. \text{ If } (2k_0 - 1)\, \Delta/2 < -1, \text{ then } \beta_1 = 1 - (1 - 2k_0)^2 \tanh^2 \alpha_1.$$

Favier gives the following relationship as a function of distance from the location where the initial transient region is completed (x^*) for the rest of the solidification distance for a sample with total length L:

$$C_s(x) = C_s(x^*) + k(\Delta)/(1 - k(\Delta))[1 - C_s(x^*)][((L - x)/(L - x^*))^{(k(\Delta)-1)} - 1]$$

Figure 6(a) compares the experimentally observed longitudinal macrosegregation with that predicted from the Favier[17,18] model for the bulk and the capillary samples examined in this study. It plots the concentration ratio C_s/C_0 as a function of fraction distance solidified. The open symbols are for the 7-mm-diameter sample grown in the presence of 0.4 T transverse magnetic field. The lines correspond to the predicted macrosegregation behavior for the various Δ values, 0.25, 0.5, 1, 2, 3, and 4. It is apparent that decreasing ampoule diameter corresponds to an increasing value of Δ, *i.e.*, an increasing diffusive and decreasing convective mass transport. However, there is significant convection present even in the 1-mm-diameter ampoule. It is also apparent that 0.4 T transverse magnetic field has little influence on the extent of convection.

A detailed comparison of experimental observations to Favier's model with a small increment in the parameter Δ, at intervals of 0.05, was carried out to identify the two

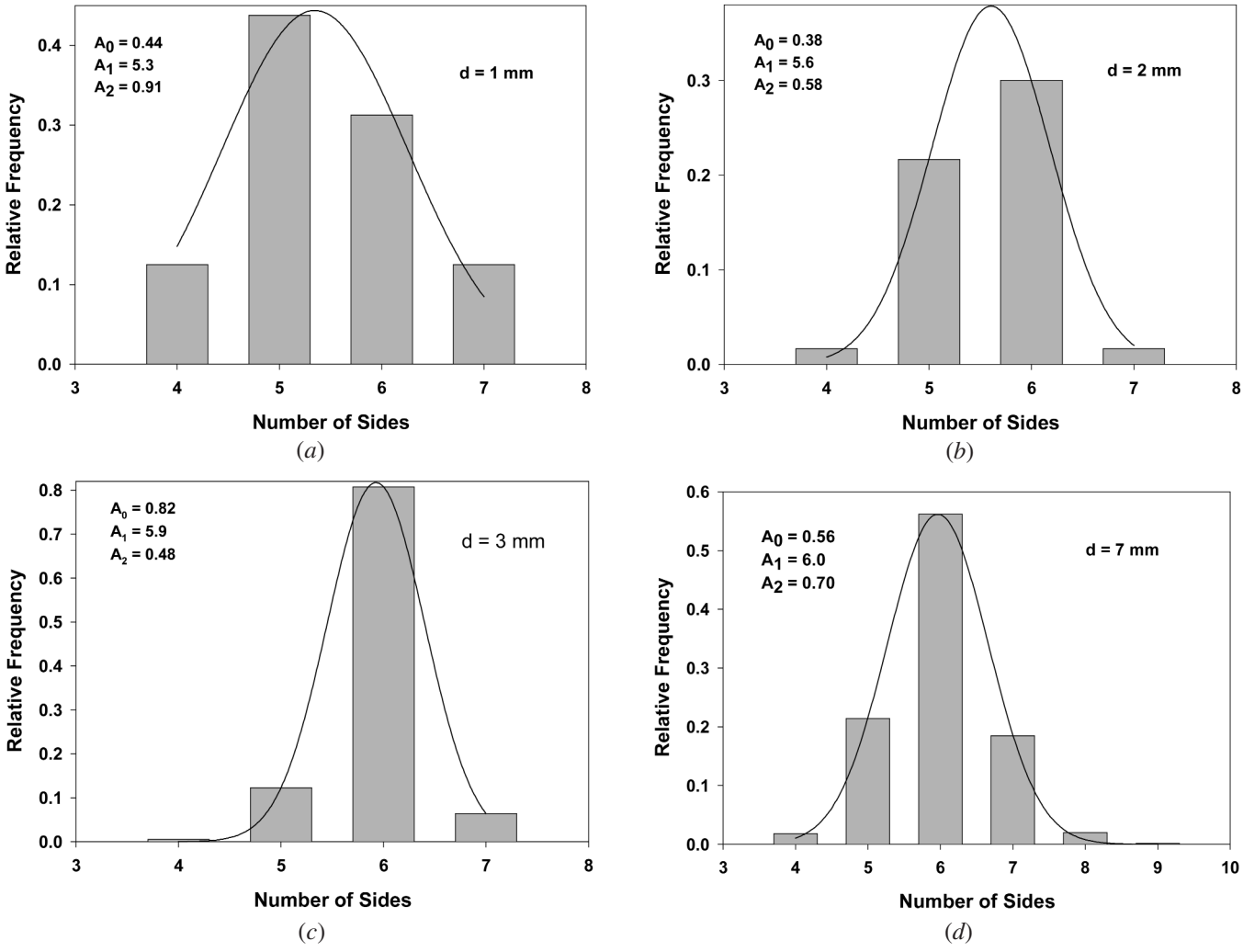

Fig. 4—Influence of reducing the ampoule diameter on the ordering of primary dendrites. Frequency distribution of the number of nearest neighbor dendrites on the transverse sections. The solid lines correspond to the Gaussian fit to the data: (*a*) 1-mm diameter, (*b*) 2-mm diameter, (*c*) 3-mm diameter, (*d*) 7-mm diameter.

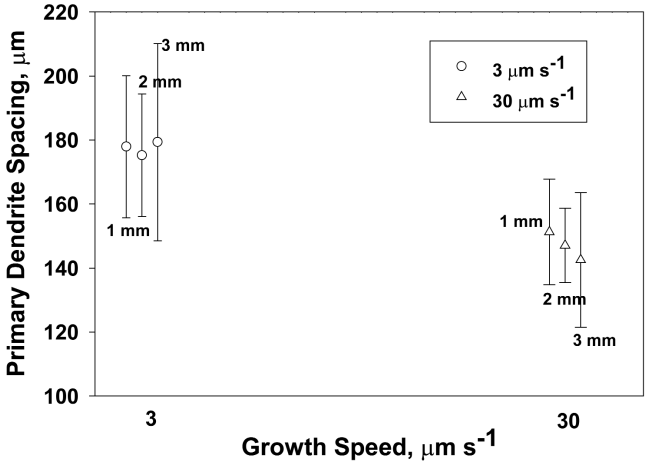

Fig. 5—Effect of growth speed and the ampoule diameter on the primary dendrite spacing as obtained from minimum spanning tree analysis.

closest Δ values that provide the best fit to the experimental macrosegregation data since the data did not show an exact match with specific theoretical curves. These Δ values are plotted in Figure 6(b) as a function of ampoule diameter (*d*). A regression analysis with 95 pct confidence interval shows that $\ln(\Delta) = -0.22 - 0.50 \ln(d, \text{mm})$ with $R^2 = 0.90$. Assuming that a Δ value of 4 is required for a dominant diffusive mass transport, an extrapolation of the above Δ *vs* ampoule diameter relationship yields the corresponding ampoule diameter to be 40 μm. This suggests that diffusive mass transport requires 40-μm-diameter capillary. Since the primary dendrite spacing itself is about 150 to 200 μm, growth in a 40-μm-diameter crucible will not allow a dendrite array to develop. It will also introduce significant wall-effect constraints on the morphology of growing dendrite.

An ampoule diameter of 1 mm was small enough to suppress convection during directional solidification of Al-4 wt pct Cu alloy.[8,9] Apparently, the convection during directional solidification of solutally stable Al-4 wt pct Cu that arises mainly from the small radial thermal gradients near the liquid-solid interface is less intense compared with the convection that occurs during growth of solutally unstable Pb-2.2 wt pct Sb alloy.

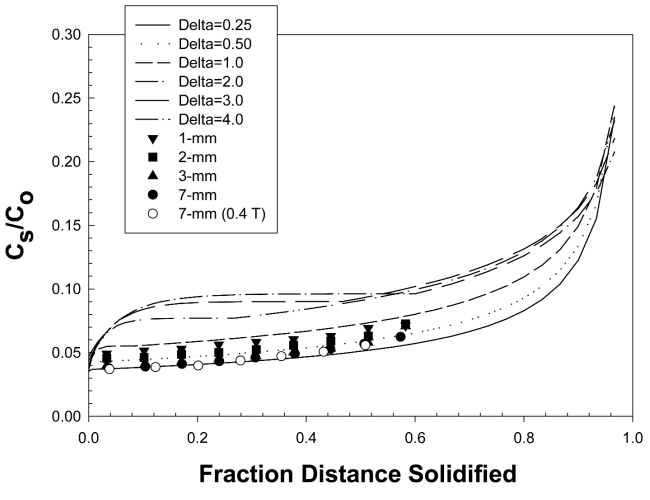

(*a*)

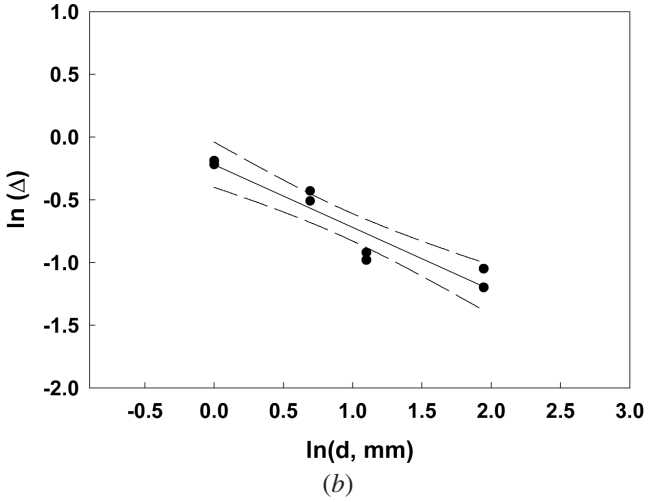

(*b*)

Fig. 6—Comparison of the longitudinal macrosegregation with varying Δ values used in the Favier's model.[17,18] (*a*) C_s/C_0 as a function of fraction distance solidified. (*b*) Effect of reducing the ampoule diameter on the convection parameter Δ. The open and closed symbols are the two approximate values for each diameter; the solid line is the fitted curve: ln (Δ) = −0.22 − 0.50 ln (diameter, mm) with $R^2 = 0.90$. The dashed lines indicate the 95 pct confidence interval.

V. CONCLUSIONS

The following conclusions can be drawn from this study, where Pb-2.2 wt pct Sb has been directionally solidified in 1-, 2-, 3-, and 7-mm-diameter crucibles with planar (thermal gradient = 82 and 120 K cm^{-1}, and growth speed = 0.4 μm s^{-1}) and dendritic (thermal gradient = 82 K cm^{-1}, and growth speed = 3 and 30 μm s^{-1}) liquid-solid interface morphologies.

1. Convection during directional solidification with a planar liquid-solid interface produces extensive longitudinal macrosegregation. Application of a 0.4 T transverse magnetic field has no effect on the extent of this convection or segregation.
2. The longitudinal macrosegregation relationship proposed by Favier[17,18] appears to fit the experimentally observed behavior by suitably adjusting the value of the parameter $\Delta = \delta R/D_l$, where δ is the momentum boundary layer thickness, R, the growth speed, and D_l, the solutal diffusivity in the melt.
3. Reducing the ampoule diameter (d) decreases the extent of convection, the relationship being ln (Δ) = −0.22 − 0.5 ln (d, mm). By extrapolating this relationship, it would appear that the diffusive transport condition ($\Delta \geq 4$) would require directional solidification in 40-μm-diameter capillaries. However, it is too small a diameter to grow dendrite arrays which usually have 150- to 200-μm primary spacing.
4. Reduction of the crucible diameter from 7 to 1 mm does not have any significant effect on the primary dendrite spacing. However, growth in the small diameter crucible, especially the 1 mm, results in significant distortion of the dendrites and increased dendrite disorder.

ACKNOWLEDGMENTS

This research was supported by the Microgravity Materials Science Program at the NASA–Marshall Space Flight Center (Huntsville, AL).

REFERENCES

1. S.H. Davis: in *Handbook of Crystal Growth I Fundamentals, Part B: Transport and Stability*, D.T.J. Hurle, ed., North-Holland, Amsterdam, 1993, pp. 859-97.
2. S.R. Coriell, B.T. Murray, A.A. Chernov, and G.B. McFadden: *Metall. Mater. Trans. A*, 1996, vol. 27A, pp. 687-94.
3. J.J. Favier and A. Rouzad: *J. Cryst. Growth*, 1987, vol. 64, pp. 367-72.
4. S.N. Tewari and M.A. Chopra: *J. Cryst. Growth*, 1992, vol. 118, pp. 183-92.
5. H. Yu, K.N. Tandon, and J.R. Cahoon: *Metall. Mater. Trans. A*, 1997, vol. 28A, pp. 1245-50.
6. M.D. Dupouy, D. Camel, and J.J. Favier: *Acta Metall. Mater.*, 1992, vol. 40, pp. 1791-99.
7. T. Okamoto, K. Kishitake, and I. Bessho: *J. Crystal Growth*, 1975, vol. 29, pp. 131-36.
8. R. Trivedi, H. Miyahara, P. Mazumder, E. Simsek, and S.N. Tewari: *J. Cryst. Growth*, 2000, vol. 222, pp. 365-79.
9. R. Trivedi, S. Liu, P. Mazumder, and E. Simsek: *Sci. Technol. Adv. Mater.*, 2001, vol. 2, pp. 309-20.
10. S.N. Ojha, G. Ding, Y. Lu, J. Reye, and S.N. Tewari: *Metall. Mater. Trans. A*, 1999, vol. 30A, pp. 2167-71.
11. S.N. Tewari and R. Shah: *Metall. Mater. Trans. A*, 1992, vol. 23A, pp. 3383-92.
12. S.N. Tewari, R. Shah, and H. Song: *Metall. Mater. Trans. A*, 1994, vol. 25A, pp. 1535-44.
13. *Metals Handbook*, ASM, Metals Park, OH, 1973, vol. 8, p. 329.
14. K. Niwa, M. Shimoji, S. Kado, Y. Watanabe, and T. Yokokawa: *Trans. AIME*, 1957, vol. 209, pp. 96-101.
15. S.N. Tewari, Y.H. Weng, G.L. Ding, and R. Trivedi: *Metall. Mater. Trans. A*, 2002, vol 33A, pp. 1229-43.
16. J.D. Hunt and S.Z. Lu: *Metall. Mater. Trans. A*, 1996, vol. 27A, pp. 611-23.
17. J.J. Favier: *Acta Metall.*, 1981, vol. 29, pp. 197-204.
18. J.J. Favier: *Acta Metall.*, 1981, vol. 29, pp. 205-14.